PROCEEDINGS OF SCIENCE

The cosmic ray energy spectrum measured using the Pierre Auger Observatory

Francesco Fenu[*ab] **for the Pierre Auger Collaboration**[c]

[a] *Università degli studi di Torino, Via Pietro Giuria 1, 10152 Torino, Italy*
[b] *INFN Torino, Via Pietro Giuria 1, 10152 Torino, Italy*
[c] *Observatorio Pierre Auger, Av. San Martín Norte 304, 5613 Malargüe, Argentina*
E-mail: auger_spokespersons@fnal.gov
Full author list: http://www.auger.org/archive/authors_icrc_2017.html

We present an update of the cosmic ray energy spectrum measured from 3×10^{17} eV to over 10^{20} eV at the Pierre Auger Observatory. This energy range is covered by combining data from the surface detector (subdividing the events into a vertical and a horizontal data set), from a denser array of stations and from hybrid events simultaneously recorded by the surface and the fluorescence detectors. Data collected to date, with a total exposure exceeding 67,000 km^2 sr yr, rely on the energy scale provided by the fluorescence detector. The spectral features, and the impact of systematic uncertainties on their significance, are discussed in detail.

35th International Cosmic Ray Conference — ICRC2017
10–20 July, 2017
Bexco, Busan, Korea

*Speaker.

© Copyright owned by the author(s) under the terms of the Creative Commons Attribution-NonCommercial-NoDerivatives 4.0 International License (CC BY-NC-ND 4.0).

PoS(ICRC2017)486

1. Introduction

The Pierre Auger Observatory [1] is the largest cosmic ray Observatory built so far. It is located in the Argentinian pampa near Malargüe, Mendoza province and has been in operation since 2004. The cosmic rays are studied by combining the measurements of a Surface Detector (SD) and a Fluorescence Detector (FD). The SD consists of 1600 Water Cherenkov Detectors (WCDs) on a 1500 m triangular grid (SD 1500), covering an area of $\sim$3000 km^2, and of additional 61 detectors covering 23.5 km^2 on a 750 m grid (SD 750). The SD 1500 is fully efficient at 3×10^{18} eV while the SD 750 from 3×10^{17} eV onwards. The atmosphere above the array is monitored by the 27 telescopes of the FD located in five buildings along the perimeter of the site. 24 telescopes have a field of view of $30^\circ \times 30^\circ$ in azimuth and elevation, with a minimum elevation of 1.51° above the horizon. Three additional telescopes, the High Elevation Auger Telescopes, can cover an elevation up to 60° to detect the low energy showers in coincidence with the SD 750. The FD measurements provide an almost calorimetric estimate of the shower energy but are limited by the atmospheric conditions while the SD measurements are made nearly 100% of the time. The main advantage of a hybrid system that combines the FD and SD measurements is the good control of the systematic uncertainties in the energy scale. It is possible calibrate the SD signal by exploiting the events where a simultaneous measurement of SD signal and FD energy is made, thus largely avoiding the use of Monte Carlo to reconstruct the energy.

In this contribution we present the energy spectrum measured at the Pierre Auger Observatory using an exposure exceeding 67,000 km^2 sr yr cumulated since January 2004 until December 2016. The measurements benefit from an improved reconstruction of the FD and SD events which will be described in detail.

2. Improvements in the event reconstruction

An accurate reconstruction of the FD events is complex, since it requires the knowledge of parameters like the fluorescence yield, the atmospheric conditions, the absolute calibration of the telescopes and many others. The entire procedure allows us to reconstruct the longitudinal profile of the energy deposit (dE/dX) of the air shower in the atmosphere. Finally, from $E_{\rm cal} = \int (dE/dX)\, dX$, which represents the energy deposited by the shower in atmosphere, the total energy is obtained by adding the so–called invisible energy, which is the energy carried into the ground by high energy muons and neutrinos. The analysis used to obtain the Auger energy scale and the estimate of its systematic uncertainties has been presented in [2]. Since this work, we have refined the reconstruction of the FD events obtaining an improved determination of the shower energies.

The reconstruction technique of the central laser facility of the Observatory, used to obtain the hourly measurements of the vertical aerosol optical depth, has improved, and now accounts for the shape of the aerosol scattering phase function and for the multiple scattering in the atmosphere. The two improvements cause an increase in the aerosol optical depth and consequently the shower energy increases of about 1% to 3% [3].

We have also improved the calibration of the FD telescopes. In the previous estimation, the optical efficiency, which is the relative FD response at various wavelengths, was the same for all telescopes. Now, after a dedicated campaign of measurements, we use the optical efficiency

PoS(ICRC2017)486

appropriate to each telescope which allows us to correctly take into account the different materials of which the mirrors are made [4]. We furthermore improved the estimation of the photomultiplier calibration constants used for the first years of data taking, during the construction phase of the Observatory. The shower energy is only marginally affected by all the improvements in the detector modelling with an average increase of 1%.

Another improvement concerns the reconstruction of the longitudinal profiles of the showers. The measured dE/dX is fitted using a Gaisser–Hillas (GH) function, but when only part of the energy deposited is detected, the extrapolation of the GH profile beyond the range of the measurements can introduce significant uncertainties in the determination of the electromagnetic shower energy. This happens in the showers of low energy ($< 10^{18}$ eV), for which only the flux of photons coming from the atmospheric depths around the profile maximum is bright enough to dominate over the night sky background. This problem has been solved by introducing a Gaussian constraint on the ratio $k = \frac{E_{\rm cal}}{(dE/dX)_{\rm max}}$ in the likelihood minimization procedure to fit the dE/dX profile, where $(dE/dX)_{\rm max}$ is the energy deposited close to the maximum. The value of the constraint has been parameterised as a function of $E_{\rm cal}$ using an average of the QGSJetII–04 [5], EPOS–LHC [6], Sibyll2.3 [7] predictions with a mixed proton and iron composition and has been set to $k = (332.6 + 13.67\ \log_{10} E_{\rm cal})\ {\rm g/cm^2}$. The uncertainty σ_k is calculated as the standard deviation of k, taking into account the different models used and the different composition simulated, and amounts to 29 ${\rm g/cm^2}$. Both the parameter k and σ_k are used in the likelihood function to constrain the GH fit. The new constraint improves the reconstruction of the low energy events, while its effect becomes negligible at energies $> 10^{18}$ eV. A more precise determination of the shower axis and a better pixel selection is also performed leading to a decrease in the shower energy by less than 1%.

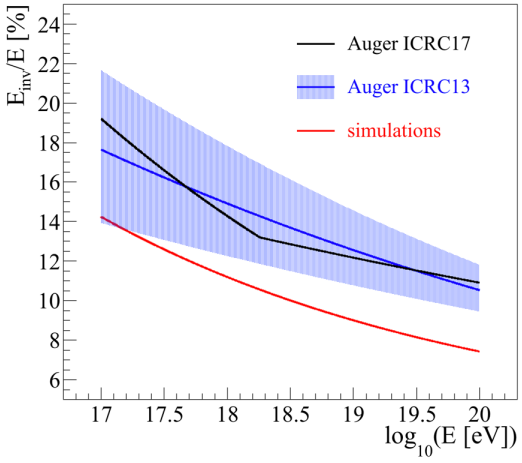

Figure 1: Ratio of the invisible energy to the total shower energy as a function of energy. The new Auger estimation (ICRC17) is compared with the previous parameterisation (ICRC13) [8] (the shaded band represents its systematic uncertainty) and with the one obtained by simulations.

The estimation of the invisible energy ($E_{\rm inv}$) has been also improved. Our previous estimate was derived from events detected simultaneously by the FD and SD detectors (hybrid events) with zenith angles below 60° [8]. In this work, $E_{\rm inv}$ is estimated from the SD events with zenith angles between 60° and 80° and with energies above 4×10^{18} eV [9]. The advantage of using these showers is that the electromagnetic component is largely absorbed by the atmosphere and the signal in the SD detectors is dominated by muons. The estimator of the muon content in the shower R_μ [10] is well correlated with $E_{\rm inv}$ through a power law function $E_{\rm inv} = C\ R_\mu^\delta$. The coefficients C and δ have been determined using the QGSJetII–04 interaction model with a mixed composition of protons and iron nuclei ($C = 0.71 \times 10^{18}$ eV and $\delta = 0.96$) and then used to estimate $E_{\rm inv}$ from

PoS(ICRC2017)486

the measurements of R_μ. In this way, most of the systematic uncertainties in $E_{\rm inv}$ related to the predictions of the muon size are avoided. To extend the invisible energy evaluation to events below 60°, $E_{\rm inv}$ is parameterised as a function of $E_{\rm cal}$ based on an analysis of the hybrid events. This parameterisation is valid only above 4×10^{18} eV where the R_μ measurements are performed. The extrapolation to lower energies is obtained taking into account the evolution with energy of the mean mass composition measured at the Auger Observatory[11]. This is done using model–based functions with parameters that have been fixed to match the measurements at higher energies, finally obtaining:

$$E_{\rm inv} = f_\theta a \left(\frac{E_{\rm cal}}{10^{18}\ {\rm eV}}\right)^b \times 10^{18}\ {\rm eV} \qquad E_{\rm cal} > E^A_{\rm cal}$$

$$E_{\rm inv} = f_\theta\ a \left(\frac{E^A_{\rm cal}}{10^{18}\ {\rm eV}}\right)^b \left(\frac{E_{\rm cal}}{E^A_{\rm cal}}\right)^{b_{\rm extr}} \times 10^{18}\ {\rm eV} \qquad E_{\rm cal} < E^A_{\rm cal}$$

where $a = 0.1633$, $b = 0.9463$, $b_{\rm extr} = 0.8475$. $E^A_{\rm cal} = 1.67\times10^{18}$ eV is the energy at which the measurements made at the Observatory show a break in the elongation rate of the slant depth of the shower maximum ($X_{\rm max}$) and $f_\theta = 0.957$ is a factor that allows us to get an unbiased $E_{\rm inv}$ estimation for the majority of the events with zenith angles $\theta < 60°$, given that the invisible energy tends to be larger for showers at larger zenith angles. The new $E_{\rm inv}$ estimation is shown in Fig.1. It is fully consistent with our previous measurements, the only difference being the slope. The change arises from the improved sensitivity to the evolution of the mass composition with energy. The difference between our estimate and the one obtained using Monte Carlo (shown in Fig.1 by the red line) is a consequence of the well–known deficit of muons in the simulations, demonstrated in various analyses of the Auger data [12][13].

With the improved reconstruction presented in this paper, the cumulative energy shift of the FD energies is slightly energy dependent (larger at higher energies) and below 4%. The total uncertainty of 14% in the energy scale and the uncertainties estimated for each sector of the reconstruction [2] are not significantly affected by the improvements in the FD reconstruction discussed above.

3. The energy spectrum from SD 1500 events under 60 degrees

The energy estimator of the SD events with zenith angles below 60° is based on the lateral distribution of secondary particles on ground at an optimal distance from the shower core. For the SD 1500, the optimal distance is determined empirically and is 1000 m. The seasonal and diurnal variations in the atmospheric parameters affect the distribution of the charged particles on ground and therefore the energy estimators. Such effects are corrected by modelling the dependence of the signal on the atmospheric parameters [14]. The presence of the geomagnetic field is accounted for [15].

Because of the attenuation of the shower when crossing the atmosphere, S(1000) decreases with zenith angle for a given energy. Assuming an isotropic flux of cosmic rays, this dependence can be removed by using the Constant Intensity Cut method [16] converting S(1000) to the equivalent signal at median zenith angle of 38° (S_{38}).

PoS(ICRC2017)486

The correlation between the SD energy estimator S_{38} and the calorimetric energy $E_{\rm FD}$, measured by the FD, can be well described by a simple power law function $E_{FD} = A(S_{38})^B$ [17]. The parameters A and B are obtained through a fit on a sub–sample of high quality hybrid events in the energy range of full efficiency of the SD.

The events are selected if the detector with the highest signal is enclosed in an hexagon of 6 active stations and the exposure is obtained geometrically [18]. A first estimate of the flux (the raw flux) is then obtained.

Finite energy resolution and the consequent bin migration, are accounted for using a forward folding procedure. The result is an energy dependent factor $C(E)$, which is the correction to be applied to the raw flux $J_{\rm unfolded} = C(E)J_{\rm raw}$. The correction to the flux by this procedure is of the order of 8% at 3×10^{18} eV, 1% at 10^{19} eV and 10% at 10^{20} eV.

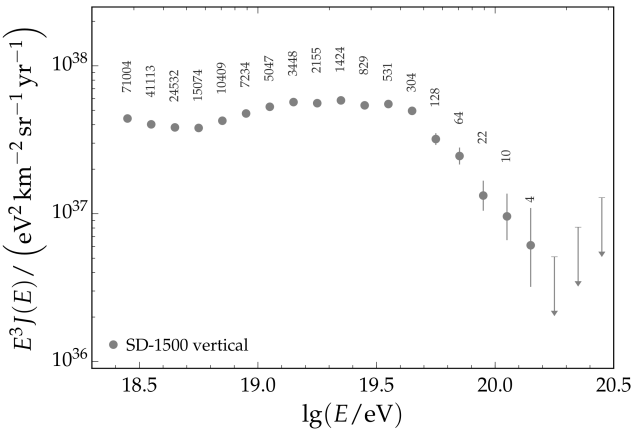

Figure 2: The unfolded spectrum for the SD 1500 vertical sample. The number of events is shown for each bin. The error bars represent statistical uncertainties. The upper limits correspond to the 84% C.L.

The SD 1500 vertical spectrum shown here includes data from January 2004 to December 2016, with a total exposure of 51,588 km^2 sr yr (roughly 20% higher than [19]). Several quality cuts are required: space–time coincidence of at least 3 neighboring triggering stations, containment of the events into an active hexagon and successful reconstruction of the lateral distribution of the events. Events detected in periods with problems in communication systems or in the vicinity of lightnings are excluded.

A total of 183,332 events with zenith angles below 60° and energies above 3×10^{18} eV is selected. The spectrum is shown in Fig. 2 where we clearly see the ankle around 5×10^{18} eV and a steepening at the highest energies.

The events collected in the SD 1500 vertical spectrum cover a wide range of declinations from $-90°$ to 25° (more than 70% of the sky). This, along with the large cumulated exposure, can be exploited to investigate possible dependences of the spectrum on the declination. Data have been divided in two declination bands, (-90°,-15.7°) (south) and (-15.7°,25°) (north) and the spectrum has been evaluated for each sample. This choice also allows us to compare the spectrum measured by the Pierre Auger Observatory with the one by Telescope Array in the common declination band [20].

We show in Fig.3 (left) the spectrum divided in declination bands together with the overall one; the residuals with respect to the overall spectrum are plotted in the right panel.

PoS(ICRC2017)486

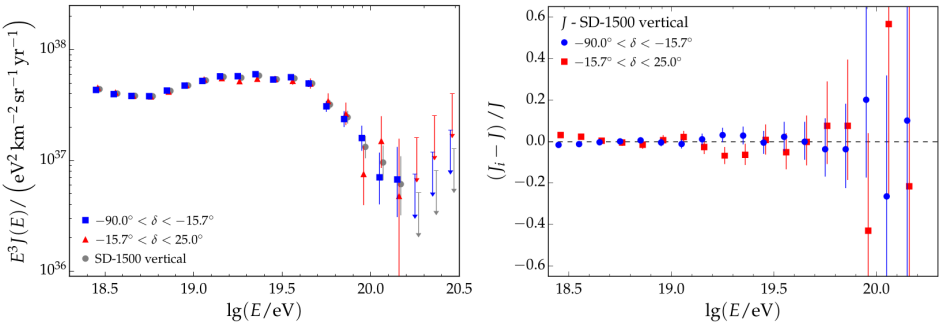

Figure 3: Left panel: The spectrum in declination bands (blue and red points), compared to the overall one (in gray). Right panel: the residual of the spectra in the various declination bands with respect to the overall spectrum.

4. Other measurements of the energy spectrum

Different data samples (see Tab.1 for their parameters) can be used from the Pierre Auger Observatory to derive the energy spectrum. Similar approaches are used to obtain each of the spectra but there are minor differences. The SD 750 energy estimator is the signal measured at 450 m from the core, S(450), corrected to a reference zenith angle of 35°, S_{35}. The SD 1500 events with zenith angles above 60° are reconstructed with an estimation of the relative muon content N_{19} with respect to a simulated proton shower with energy 10^{19} eV [10]. Finally, the hybrid sample is built from events detected by the FD simultaneously with at least one detector of the SD 1500. The hybrid exposure is calculated using a detailed Monte Carlo simulation [21].

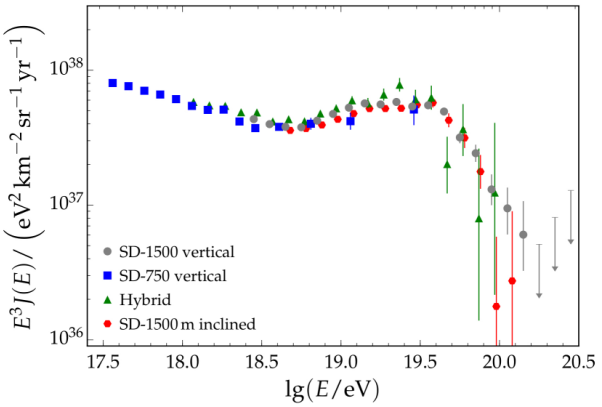

Figure 4: The energy spectra obtained with SD 1500 vertical, inclined, hybrid and SD 750 events are shown here. The systematic uncertainty on the energy scale, common to all of them, is 14%

The SD 1500 spectra obtained with events below and above 60°, the SD 750 and the hybrid spectra are shown together in Fig.4.

All the spectra agree within the systematic uncertainties, which are dominated by the energy scale one (14%). The systematic uncertainties on the flux are between 5 and 10% and are responsible for the difference in normalization between the spectra visible in Fig.4.

A combined spectrum is obtained by means a maximum likelihood fit. The likelihood function is defined in such a way as to fit all the four data sets globally. The flux normalizations are used as additional constraints to obtain the flux scaling factors that match them: (-0.8±0.2)% for the SD 1500 vertical, (-1± 4)% for the SD 750, (5.4± 0.7)% for the SD 1500 horizontal and (-6 ± 2)% for the hybrid.

PoS(ICRC2017)486

	SD 1500 $< 60^\circ$	SD 1500 $> 60^\circ$	SD 750	Hybrid
Data taking period	Jan. 2004 – Dec. 2016	Jan. 2004 – Dec. 2016	Aug. 2008 – Dec. 2016	Jan. 2007 – Dec 2015
Exposure [km^2 sr yr]	51,588	15,121	228	1946 @10^{19} eV
Number of events	183,332	19,602	87,402	11,680
Zenith angle range [deg.]	0–60	60–80	0–55	0–60
Energy threshold [eV]	3×10^{18}	4×10^{18}	3×10^{17}	10^{18}
Calibration parameters				
Number of events	2661	312	1276	
A [eV]	$(1.78\pm0.03)\times10^{17}$	$(5.45\pm0.08)\times10^{18}$	$(1.4\pm0.04)\times10^{16}$	
B	1.042 ± 0.005	1.030 ± 0.018	1.000 ± 0.008	
Energy resolution [%]	15	17	13	

Table 1: The parameters of the data samples presented here together with the calibration parameters.

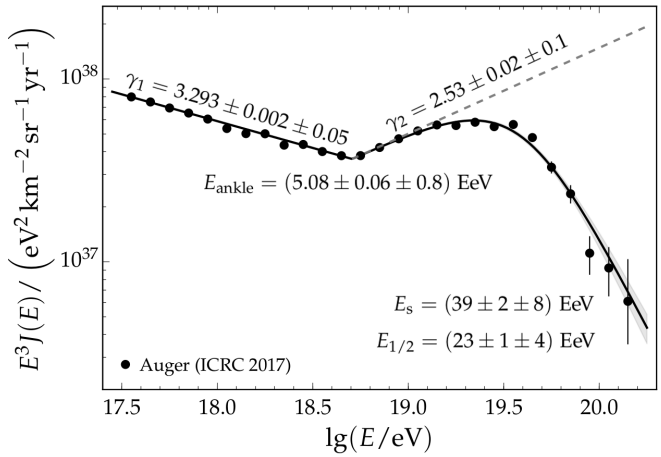

Figure 5: The combined spectrum and the fitting function with the fitting parameters.

To obtain the spectral parameters, the combined spectrum is fitted with the function:

$$J_{\rm unf}(E) = \begin{cases} J_0\left(\frac{E}{E_{\rm ankle}}\right)^{-\gamma_1} & E < E_{\rm ankle} \\ J_0\left(\frac{E}{E_{\rm ankle}}\right)^{-\gamma_2}\left[1+\left(\frac{E_{\rm ankle}}{E_{\rm s}}\right)^{\Delta\gamma}\right]\left[1+\left(\frac{E}{E_{\rm s}}\right)^{\Delta\gamma}\right]^{-1} & E > E_{\rm ankle} \end{cases} \tag{4.1}$$

The spectrum, the fit and the optimized parameters are plotted in Fig.5. An ankle is found at $E_{\rm ankle} = (5.08\pm0.06(\text{stat.})\pm0.8(\text{syst.}))\times10^{18}$ eV, while the suppression is at $E_s = (3.9\pm0.2(\text{stat.})\pm 0.8(\text{syst.}))\times10^{19}$ eV. The energy $\mathrm{E}_{1/2}$ at which the integral spectrum drops by a factor of two below what would be the expected with no steepening is $\mathrm{E}_{1/2} = (2.26\pm0.08(\text{stat.})\pm0.4(\text{syst.}))\times10^{19}$ eV. The spectral indexes are: $\gamma_1 = 3.293\pm0.002(\text{stat.})\pm0.05(\text{syst.})$, $\gamma_2 = 2.53\pm0.02(\text{stat.})\pm 0.1(\text{syst.})$ while $\Delta\gamma = 2.5\pm0.1(\text{stat.})\pm0.4(\text{syst.})$.

5. Summary

We have presented an update of the energy spectrum above 3×10^{17} eV as obtained using the Pierre Auger Observatory. An improved FD reconstruction caused an increase in the FD energy of less than 4%, while the systematic uncertainties previously estimated by the Auger Collaboration

PoS(ICRC2017)486

are confirmed. The SD 1500 vertical spectrum has been obtained with unprecedented precision based on an exposure of more than 51,000 km^2 sr yr. A study of the declination dependence of the spectrum showed no significant north–south asymmetry.

The combined spectrum from four different data sets has been derived using data collected by the Pierre Auger Observatory over more than 10 years (cumulating 67,000 km^2 sr yr of exposure). The measured cosmic ray flux is well described by a broken power law plus a smooth suppression at the highest energies. The dominant systematic uncertainty stems from the overall uncertainty in the energy scale of 14%. The obtained spectral parameters are in good agreement with those previously shown [19].

References

[1] The Pierre Auger Collaboration, *Nucl. Instrum. Meth. A* **798** (2015) 172.

[2] V. Verzi for the Pierre Auger Collaboration, *Proc. 33th ICRC 2013*, Rio de Janeiro, Brazil [arXiv:1307.5059].

[3] M. Malacari for the Pierre Auger Collaboration, Proc 35th ICRC 2017, this conference.

[4] B. Gookin, doctoral thesis, https://dspace.library.colostate.edu/bitstream/handle/10217/167192/Gookin_colostate_0053A_13168o.pdf?sequence=4&isAllowed=y

[5] S. Ostapchenko, *Phys. Rev. D* 83 (2011) 014018.

[6] T. Pierog, *Phys. Rev. C* 92 (2015) 034906.

[7] F. Riehn, *Proc. 34th ICRC 2015*, The Hague, The Netherlands [arXiv:1510.00568].

[8] M. Tueros for the Pierre Auger Collaboration, *Proc. 33th ICRC 2013*, Rio de Janeiro, Brazil [arXiv:1307.5059]

[9] A. Mariazzi for the Pierre Auger Collaboration, *Proc. of the 2016 Conference on Ultrahigh Energy Cosmic Rays*, Kyoto, Japan (2016), in press.

[10] The Pierre Auger Collaboration, *JCAP* **08** (2014) 019.

[11] A. Porcelli for the Pierre Auger Collaboration, *Proc. 34th ICRC 2015*, The Hague, The Netherlands. PoS(ICRC2015)420.

[12] The Pierre Auger Collaboration, *Phys. Rev. D* 91, 032003 (2015)

[13] The Pierre Auger Collaboration, *Phys. Rev. Lett.* 117 (2016) 192001.

[14] The Pierre Auger Collaboration, *JINST* 12 (2017) P02006.

[15] The Pierre Auger Collaboration, *JCAP11* (2011) 022.

[16] J. Hersil et al., *Phys. Rev. Lett.* 6 (1961) 22.

[17] R. Pesce for the Pierre Auger Collaboration, *Proc. 32nd ICRC 2011*, Beijing, China, DOI: 10.7529/ICRC2011/V02/1160.

[18] The Pierre Auger Collaboration, *Nucl. Instrum. Meth. A* 613 (2010) 29.

[19] I. Valiño for the Pierre Auger Collaboration, *Proc. 34th ICRC 2015*, The Hague, The Netherlands. PoS(ICRC2015)271.

[20] D. Ivanov for the Pierre Auger and Telescope Array collaborations, *Proc. 35th ICRC 2017*, this conference

[21] The Pierre Auger Collaboration, *Astropart. Phys.* 34 (2011) 368–381.

PoS(ICRC2017)486

The Pierre Auger Collaboration

A. Aab[77], P. Abreu[69], M. Aglietta[50,49], I.F.M. Albuquerque[18], I. Allekotte[1], A. Almela[8,11], J. Alvarez Castillo[65], J. Alvarez-Muñiz[76], G.A. Anastasi[41,43], L. Anchordoqui[83], B. Andrada[8], S. Andringa[69], C. Aramo[47], N. Arsene[71], H. Asorey[1,27], P. Assis[69], J. Aublin[32], G. Avila[9,10], A.M. Badescu[72], A. Balaceanu[70], F. Barbato[57], R.J. Barreira Luz[69], K.H. Becker[34], J.A. Bellido[12], C. Berat[33], M.E. Bertaina[59,49], X. Bertou[1], P.L. Biermann[b], J. Biteau[31], S.G. Blaess[12], A. Blanco[69], J. Blazek[29], C. Bleve[53,45], M. Boháčová[29], D. Boncioli[43,g], C. Bonifazi[24], N. Borodai[66], A.M. Botti[8,36], J. Brack[f], I. Brancus[70], T. Bretz[38], A. Bridgeman[35], F.L. Briechle[38], P. Buchholz[40], A. Bueno[75], S. Buitink[77], M. Buscemi[55,44], K.S. Caballero-Mora[63], B. Caccianiga[46], L. Caccianiga[56], A. Cancio[11,8], F. Canfora[77], L. Caramete[71], R. Caruso[55,44], A. Castellina[50,49], F. Catalani[16], G. Cataldi[45], L. Cazon[69], A.G. Chavez[64], J.A. Chinellato[19], J. Chudoba[29], R.W. Clay[12], A. Cobos[8], R. Colalillo[57,47], A. Coleman[87], L. Collica[49], M.R. Coluccia[53,45], R. Conceição[69], G. Consolati[46], G. Consolati[46,51], F. Contreras[9,10], M.J. Cooper[12], S. Coutu[87], C.E. Covault[81], J. Cronin[88], S. D'Amico[52,45], B. Daniel[19], S. Dasso[5,3], K. Daumiller[36], B.R. Dawson[12], R.M. de Almeida[26], S.J. de Jong[77,79], G. De Mauro[77], J.R.T. de Mello Neto[24,25], I. De Mitri[53,45], J. de Oliveira[26], V. de Souza[17], J. Debatin[35], O. Deligny[31], M.L. Díaz Castro[19], F. Diogo[69], C. Dobrigkeit[19], J.C. D'Olivo[65], Q. Dorosti[40], R.C. dos Anjos[23], M.T. Dova[4], A. Dundovic[39], J. Ebr[29], R. Engel[36], M. Erdmann[38], M. Erfani[40], C.O. Escobar[e], J. Espadanal[69], A. Etchegoyen[8,11], H. Falcke[77,80,79], J. Farmer[88], G. Farrar[85], A.C. Fauth[19], N. Fazzini[e], F. Fenu[59,49], B. Fick[84], J.M. Figueira[8], A. Filipčič[74,73], M.M. Freire[6], T. Fujii[88], A. Fuster[8,11], R. Gaïor[32], B. García[7], F. Gaté[d], H. Gemmeke[37], A. Gherghel-Lascu[70], U. Giaccari[24], M. Giammarchi[46], M. Giller[67], D. Głas[68], C. Glaser[38], G. Golup[1], M. Gómez Berisso[1], P.F. Gómez Vitale[9,10], N. González[8,36], A. Gorgi[50,49], A.F. Grillo[43], T.D. Grubb[12], F. Guarino[57,47], G.P. Guedes[20], R. Halliday[81], M.R. Hampel[8], P. Hansen[4], D. Harari[1], T.A. Harrison[12], A. Haungs[36], T. Hebbeker[38], D. Heck[36], P. Heimann[40], A.E. Herve[35], G.C. Hill[12], C. Hojvat[e], E. Holt[36,8], P. Homola[66], J.R. Hörandel[77,79], P. Horvath[30], M. Hrabovský[30], T. Huege[36], J. Hulsman[8,36], A. Insolia[55,44], P.G. Isar[71], I. Jandt[34], J.A. Johnsen[82], M. Josebachuili[8], J. Jurysek[29], A. Kääpä[34], O. Kambeitz[35], K.H. Kampert[34], B. Keilhauer[36], N. Kemmerich[18], E. Kemp[19], J. Kemp[38], R.M. Kieckhafer[84], H.O. Klages[36], M. Kleifges[37], J. Kleinfeller[9], R. Krause[38], N. Krohm[34], D. Kuempel[34], G. Kukec Mezek[73], N. Kunka[37], A. Kuotb Awad[35], B.L. Lago[15], D. LaHurd[81], R.G. Lang[17], M. Lauscher[38], R. Legumina[67], M.A. Leigui de Oliveira[22], A. Letessier-Selvon[32], I. Lhenry-Yvon[31], K. Link[35], D. Lo Presti[55], L. Lopes[69], R. López[60], A. López Casado[76], R. Lorek[81], Q. Luce[31], A. Lucero[8,11], M. Malacari[88], M. Mallamaci[56,46], D. Mandat[29], P. Mantsch[e], A.G. Mariazzi[4], I.C. Mariş[13], G. Marsella[53,45], D. Martello[53,45], H. Martinez[61], O. Martínez Bravo[60], J.J. Masías Meza[3], H.J. Mathes[36], S. Mathys[34], G. Matthiae[58,48], E. Mayotte[34], P.O. Mazur[e], C. Medina[82], G. Medina-Tanco[65], D. Melo[8], A. Menshikov[37], K.-D. Merenda[82], S. Michal[30], M.I. Micheletti[6], L. Middendorf[38], L. Miramonti[56,46], B. Mitrica[70], D. Mockler[35], S. Mollerach[1], F. Montanet[33], C. Morello[50,49], G. Morlino[41,43], M. Mostafá[87], A.L. Müller[8,36], G. Müller[38], M.A. Muller[19,21], S. Müller[35,8], R. Mussa[49], I. Naranjo[1], L. Nellen[65], P.H. Nguyen[12], M. Niculescu-Oglinzanu[70], M. Niechciol[40], L. Niemietz[34], T. Niggemann[38], D. Nitz[84], D. Nosek[28], V. Novotny[28], L. Nožka[30], L.A. Núñez[27], L. Ochilo[40], F. Oikonomou[87], A. Olinto[88], M. Palatka[29], J. Pallotta[2], P. Papenbreer[34], G. Parente[76], A. Parra[60], T. Paul[83], M. Pech[29], F. Pedreira[76], J. Pękala[66], R. Pelayo[62], J. Peña-Rodriguez[27], L. A. S. Pereira[19], M. Perlin[8], L. Perrone[53,45], C. Peters[38], S. Petrera[41,43], J. Phuntsok[87], R. Piegaia[3], T. Pierog[36], M. Pimenta[69], V. Pirronello[55,44], M. Platino[8], M. Plum[38], J. Poh[88], C. Porowski[66], R.R. Prado[17], P. Privitera[88], M. Prouza[29], E.J. Quel[2], S. Querchfeld[34], S. Quinn[81], R. Ramos-Pollan[27], J. Rautenberg[34], D. Ravignani[8], J. Ridky[29], F. Riehn[69], M. Risse[40], P. Ristori[2], V. Rizi[54,43], W. Rodrigues de Carvalho[18], G. Rodriguez Fernandez[58,48], J. Rodriguez Rojo[9], M.J. Roncoroni[8], M. Roth[36], E. Roulet[1], A.C. Rovero[5], P. Ruehl[40], S.J. Saffi[12], A. Saftoiu[70],

F. Salamida[54,43], H. Salazar[60], A. Saleh[73], G. Salina[48], F. Sánchez[8], P. Sanchez-Lucas[75], E.M. Santos[18], E. Santos[8], F. Sarazin[82], R. Sarmento[69], C. Sarmiento-Cano[8], R. Sato[9], M. Schauer[34], V. Scherini[45], H. Schieler[36], M. Schimp[34], D. Schmidt[36,8], O. Scholten[78,c], P. Schovánek[29], F.G. Schröder[36], S. Schröder[34], A. Schulz[35], J. Schumacher[38], S.J. Sciutto[4], A. Segreto[42,44], R.C. Shellard[14], G. Sigl[39], G. Silli[8,36], R. Šmída[36], G.R. Snow[89], P. Sommers[87], S. Sonntag[40], J. F. Soriano[83], R. Squartini[9], D. Stanca[70], S. Stanič[73], J. Stasielak[66], P. Stassi[33], M. Stolpovskiy[33], F. Strafella[53,45], A. Streich[35], F. Suarez[8,11], M. Suarez Durán[27], T. Sudholz[12], T. Suomijärvi[31], A.D. Supanitsky[5], J. Šupík[30], J. Swain[86], Z. Szadkowski[68], A. Taboada[36], O.A. Taborda[1], V.M. Theodoro[19], C. Timmermans[79,77], C.J. Todero Peixoto[16], L. Tomankova[36], B. Tomé[69], G. Torralba Elipe[76], P. Travnicek[29], M. Trini[73], R. Ulrich[36], M. Unger[36], M. Urban[38], J.F. Valdés Galicia[65], I. Valiño[76], L. Valore[57,47], G. van Aar[77], P. van Bodegom[12], A.M. van den Berg[78], A. van Vliet[77], E. Varela[60], B. Vargas Cárdenas[65], R.A. Vázquez[76], D. Veberič[36], C. Ventura[25], I.D. Vergara Quispe[4], V. Verzi[48], J. Vicha[29], L. Villaseñor[64], S. Vorobiov[73], H. Wahlberg[4], O. Wainberg[8,11], D. Walz[38], A.A. Watson[a], M. Weber[37], A. Weindl[36], M. Wiedeński[68], L. Wiencke[82], H. Wilczyński[66], T. Winchen[34], M. Wirtz[38], D. Wittkowski[34], B. Wundheiler[8], L. Yang[73], A. Yushkov[8], E. Zas[76], D. Zavrtanik[73,74], M. Zavrtanik[74,73], A. Zepeda[61], B. Zimmermann[37], M. Ziolkowski[40], Z. Zong[31], F. Zuccarello[55,44]

—•—

[1] Centro Atómico Bariloche and Instituto Balseiro (CNEA-UNCuyo-CONICET), San Carlos de Bariloche, Argentina
[2] Centro de Investigaciones en Láseres y Aplicaciones, CITEDEF and CONICET, Villa Martelli, Argentina
[3] Departamento de Física and Departamento de Ciencias de la Atmósfera y los Océanos, FCEyN, Universidad de Buenos Aires and CONICET, Buenos Aires, Argentina
[4] IFLP, Universidad Nacional de La Plata and CONICET, La Plata, Argentina
[5] Instituto de Astronomía y Física del Espacio (IAFE, CONICET-UBA), Buenos Aires, Argentina
[6] Instituto de Física de Rosario (IFIR) - CONICET/U.N.R. and Facultad de Ciencias Bioquímicas y Farmacéuticas U.N.R., Rosario, Argentina
[7] Instituto de Tecnologías en Detección y Astropartículas (CNEA, CONICET, UNSAM), and Universidad Tecnológica Nacional - Facultad Regional Mendoza (CONICET/CNEA), Mendoza, Argentina
[8] Instituto de Tecnologías en Detección y Astropartículas (CNEA, CONICET, UNSAM), Buenos Aires, Argentina
[9] Observatorio Pierre Auger, Malargüe, Argentina
[10] Observatorio Pierre Auger and Comisión Nacional de Energía Atómica, Malargüe, Argentina
[11] Universidad Tecnológica Nacional - Facultad Regional Buenos Aires, Buenos Aires, Argentina
[12] University of Adelaide, Adelaide, S.A., Australia
[13] Université Libre de Bruxelles (ULB), Brussels, Belgium
[14] Centro Brasileiro de Pesquisas Fisicas, Rio de Janeiro, RJ, Brazil
[15] Centro Federal de Educação Tecnológica Celso Suckow da Fonseca, Nova Friburgo, Brazil
[16] Universidade de São Paulo, Escola de Engenharia de Lorena, Lorena, SP, Brazil
[17] Universidade de São Paulo, Instituto de Física de São Carlos, São Carlos, SP, Brazil
[18] Universidade de São Paulo, Instituto de Física, São Paulo, SP, Brazil
[19] Universidade Estadual de Campinas, IFGW, Campinas, SP, Brazil
[20] Universidade Estadual de Feira de Santana, Feira de Santana, Brazil
[21] Universidade Federal de Pelotas, Pelotas, RS, Brazil
[22] Universidade Federal do ABC, Santo André, SP, Brazil
[23] Universidade Federal do Paraná, Setor Palotina, Palotina, Brazil
[24] Universidade Federal do Rio de Janeiro, Instituto de Física, Rio de Janeiro, RJ, Brazil
[25] Universidade Federal do Rio de Janeiro (UFRJ), Observatório do Valongo, Rio de Janeiro, RJ, Brazil

[26] Universidade Federal Fluminense, EEIMVR, Volta Redonda, RJ, Brazil
[27] Universidad Industrial de Santander, Bucaramanga, Colombia
[28] Charles University, Faculty of Mathematics and Physics, Institute of Particle and Nuclear Physics, Prague, Czech Republic
[29] Institute of Physics of the Czech Academy of Sciences, Prague, Czech Republic
[30] Palacky University, RCPTM, Olomouc, Czech Republic
[31] Institut de Physique Nucléaire d'Orsay (IPNO), Université Paris-Sud, Univ. Paris/Saclay, CNRS-IN2P3, Orsay, France
[32] Laboratoire de Physique Nucléaire et de Hautes Energies (LPNHE), Universités Paris 6 et Paris 7, CNRS-IN2P3, Paris, France
[33] Laboratoire de Physique Subatomique et de Cosmologie (LPSC), Université Grenoble-Alpes, CNRS/IN2P3, Grenoble, France
[34] Bergische Universität Wuppertal, Department of Physics, Wuppertal, Germany
[35] Karlsruhe Institute of Technology, Institut für Experimentelle Kernphysik (IEKP), Karlsruhe, Germany
[36] Karlsruhe Institute of Technology, Institut für Kernphysik, Karlsruhe, Germany
[37] Karlsruhe Institute of Technology, Institut für Prozessdatenverarbeitung und Elektronik, Karlsruhe, Germany
[38] RWTH Aachen University, III. Physikalisches Institut A, Aachen, Germany
[39] Universität Hamburg, II. Institut für Theoretische Physik, Hamburg, Germany
[40] Universität Siegen, Fachbereich 7 Physik - Experimentelle Teilchenphysik, Siegen, Germany
[41] Gran Sasso Science Institute (INFN), L'Aquila, Italy
[42] INAF - Istituto di Astrofisica Spaziale e Fisica Cosmica di Palermo, Palermo, Italy
[43] INFN Laboratori Nazionali del Gran Sasso, Assergi (L'Aquila), Italy
[44] INFN, Sezione di Catania, Catania, Italy
[45] INFN, Sezione di Lecce, Lecce, Italy
[46] INFN, Sezione di Milano, Milano, Italy
[47] INFN, Sezione di Napoli, Napoli, Italy
[48] INFN, Sezione di Roma "Tor Vergata", Roma, Italy
[49] INFN, Sezione di Torino, Torino, Italy
[50] Osservatorio Astrofisico di Torino (INAF), Torino, Italy
[51] Politecnico di Milano, Dipartimento di Scienze e Tecnologie Aerospaziali , Milano, Italy
[52] Università del Salento, Dipartimento di Ingegneria, Lecce, Italy
[53] Università del Salento, Dipartimento di Matematica e Fisica “E. De Giorgi”, Lecce, Italy
[54] Università dell'Aquila, Dipartimento di Scienze Fisiche e Chimiche, L'Aquila, Italy
[55] Università di Catania, Dipartimento di Fisica e Astronomia, Catania, Italy
[56] Università di Milano, Dipartimento di Fisica, Milano, Italy
[57] Università di Napoli "Federico II", Dipartimento di Fisica “Ettore Pancini“, Napoli, Italy
[58] Università di Roma “Tor Vergata”, Dipartimento di Fisica, Roma, Italy
[59] Università Torino, Dipartimento di Fisica, Torino, Italy
[60] Benemérita Universidad Autónoma de Puebla, Puebla, México
[61] Centro de Investigación y de Estudios Avanzados del IPN (CINVESTAV), México, D.F., México
[62] Unidad Profesional Interdisciplinaria en Ingeniería y Tecnologías Avanzadas del Instituto Politécnico Nacional (UPIITA-IPN), México, D.F., México
[63] Universidad Autónoma de Chiapas, Tuxtla Gutiérrez, Chiapas, México
[64] Universidad Michoacana de San Nicolás de Hidalgo, Morelia, Michoacán, México
[65] Universidad Nacional Autónoma de México, México, D.F., México
[66] Institute of Nuclear Physics PAN, Krakow, Poland
[67] University of Łódź, Faculty of Astrophysics, Łódź, Poland

[68] University of Łódź, Faculty of High-Energy Astrophysics,Łódź, Poland
[69] Laboratório de Instrumentação e Física Experimental de Partículas - LIP and Instituto Superior Técnico - IST, Universidade de Lisboa - UL, Lisboa, Portugal
[70] "Horia Hulubei" National Institute for Physics and Nuclear Engineering, Bucharest-Magurele, Romania
[71] Institute of Space Science, Bucharest-Magurele, Romania
[72] University Politehnica of Bucharest, Bucharest, Romania
[73] Center for Astrophysics and Cosmology (CAC), University of Nova Gorica, Nova Gorica, Slovenia
[74] Experimental Particle Physics Department, J. Stefan Institute, Ljubljana, Slovenia
[75] Universidad de Granada and C.A.F.P.E., Granada, Spain
[76] Universidad de Santiago de Compostela, Santiago de Compostela, Spain
[77] IMAPP, Radboud University Nijmegen, Nijmegen, The Netherlands
[78] KVI - Center for Advanced Radiation Technology, University of Groningen, Groningen, The Netherlands
[79] Nationaal Instituut voor Kernfysica en Hoge Energie Fysica (NIKHEF), Science Park, Amsterdam, The Netherlands
[80] Stichting Astronomisch Onderzoek in Nederland (ASTRON), Dwingeloo, The Netherlands
[81] Case Western Reserve University, Cleveland, OH, USA
[82] Colorado School of Mines, Golden, CO, USA
[83] Department of Physics and Astronomy, Lehman College, City University of New York, Bronx, NY, USA
[84] Michigan Technological University, Houghton, MI, USA
[85] New York University, New York, NY, USA
[86] Northeastern University, Boston, MA, USA
[87] Pennsylvania State University, University Park, PA, USA
[88] University of Chicago, Enrico Fermi Institute, Chicago, IL, USA
[89] University of Nebraska, Lincoln, NE, USA

———

[a] School of Physics and Astronomy, University of Leeds, Leeds, United Kingdom
[b] Max-Planck-Institut für Radioastronomie, Bonn, Germany
[c] also at Vrije Universiteit Brussels, Brussels, Belgium
[d] SUBATECH, École des Mines de Nantes, CNRS-IN2P3, Université de Nantes, France
[e] Fermi National Accelerator Laboratory, USA
[f] Colorado State University, Fort Collins, CO
[g] now at Deutsches Elektronen-Synchrotron (DESY), Zeuthen, Germany

Acknowledgments

The successful installation, commissioning, and operation of the Pierre Auger Observatory would not have been possible without the strong commitment and effort from the technical and administrative staff in Malargüe. We are very grateful to the following agencies and organizations for financial support:

Argentina – Comisión Nacional de Energía Atómica; Agencia Nacional de Promoción Científica y Tecnológica (ANPCyT); Consejo Nacional de Investigaciones Científicas y Técnicas (CONICET); Gobierno de la Provincia de Mendoza; Municipalidad de Malargüe; NDM Holdings and Valle Las Leñas; in gratitude for their continuing cooperation over land access; Australia – the Australian Research Council; Brazil – Conselho Nacional de Desenvolvimento Científico e Tecnológico (CNPq); Financiadora de Estudos e Projetos (FINEP); Fundação de Amparo à Pesquisa do Estado de Rio de Janeiro (FAPERJ); São Paulo Research Foundation (FAPESP) Grants No. 2010/07359-6 and No. 1999/05404-3; Ministério de Ciência e Tecnologia (MCT); Czech Republic – Grant No. MSMT CR LG15014, LO1305, LM2015038 and CZ.02.1.01/0.0/0.0/16_013/0001402; France – Centre de Calcul IN2P3/CNRS; Centre National de la Recherche Scientifique (CNRS); Conseil Régional Ile-de-France; Département Physique Nucléaire et Corpusculaire (PNC-IN2P3/CNRS); Département Sciences de l'Univers (SDU-INSU/CNRS); Institut Lagrange de Paris (ILP) Grant No. LABEX ANR-10-LABX-63 within the Investissements d'Avenir

Programme Grant No. ANR-11-IDEX-0004-02; Germany – Bundesministerium für Bildung und Forschung (BMBF); Deutsche Forschungsgemeinschaft (DFG); Finanzministerium Baden-Württemberg; Helmholtz Alliance for Astroparticle Physics (HAP); Helmholtz-Gemeinschaft Deutscher Forschungszentren (HGF); Ministerium für Innovation, Wissenschaft und Forschung des Landes Nordrhein-Westfalen; Ministerium für Wissenschaft, Forschung und Kunst des Landes Baden-Württemberg; Italy – Istituto Nazionale di Fisica Nucleare (INFN); Istituto Nazionale di Astrofisica (INAF); Ministero dell'Istruzione, dell'Universitá e della Ricerca (MIUR); CETEMPS Center of Excellence; Ministero degli Affari Esteri (MAE); Mexico – Consejo Nacional de Ciencia y Tecnología (CONACYT) No. 167733; Universidad Nacional Autónoma de México (UNAM); PAPIIT DGAPA-UNAM; The Netherlands – Ministerie van Onderwijs, Cultuur en Wetenschap; Nederlandse Organisatie voor Wetenschappelijk Onderzoek (NWO); Stichting voor Fundamenteel Onderzoek der Materie (FOM); Poland – National Centre for Research and Development, Grants No. ERA-NET-ASPERA/01/11 and No. ERA-NET-ASPERA/02/11; National Science Centre, Grants No. 2013/08/M/ST9/00322, No. 2013/08/M/ST9/00728 and No. HARMONIA 5–2013/10/M/ST9/00062, UMO-2016/22/M/ST9/00198; Portugal – Portuguese national funds and FEDER funds within Programa Operacional Factores de Competitividade through Fundação para a Ciência e a Tecnologia (COMPETE); Romania – Romanian Authority for Scientific Research ANCS; CNDI-UEFISCDI partnership projects Grants No. 20/2012 and No. 194/2012 and PN 16 42 01 02; Slovenia – Slovenian Research Agency; Spain – Comunidad de Madrid; Fondo Europeo de Desarrollo Regional (FEDER) funds; Ministerio de Economía y Competitividad; Xunta de Galicia; European Community 7th Framework Program Grant No. FP7-PEOPLE-2012-IEF-328826; USA – Department of Energy, Contracts No. DE-AC02-07CH11359, No. DE-FR02-04ER41300, No. DE-FG02-99ER41107 and No. DE-SC0011689; National Science Foundation, Grant No. 0450696; The Grainger Foundation; Marie Curie-IRSES/EPLANET; European Particle Physics Latin American Network; European Union 7th Framework Program, Grant No. PIRSES-2009-GA-246806; European Union's Horizon 2020 research and innovation programme (Grant No. 646623); and UNESCO.

Last modified on 2017-07-31.